Simulations of Photomodulated Solute Transport in Doubly Illuminated Liquid Membranes Containing Photoactive Carriers

Teresa L. Longin,* Teresa Fraterman, and Phuong Nguyen

University of Redlands, 1200 East Colton, Redlands, California 92373-0999

Received: June 16, 2005; In Final Form: August 18, 2005

A steady-state model describing photofacilitated transport in liquid membranes under double illumination is presented. The model allows for the exploration of the effects of a wide range of thermodynamic and kinetic carrier properties on the control of photoinduced transport rates of solutes, called photomodulation. Most previous experimental and theoretical studies have explored the illumination of only the feed or sweep side of the membrane, while this study examines the effects of illuminating both sides simultaneously. Under double illumination, solute transport rates can be as much as five times greater than those measured in the dark and 2.5 times greater than rates obtained under single illumination. Carriers that are predominantly in the weakly binding form in the dark generally provide slightly better performance at lower light intensities than do carriers that are predominantly in the strongly binding form in the dark. The greatest enhancement in solute transport under double illumination is seen for carriers with very slow interconversion rate constants between the strongly and weakly binding forms. These results provide guidelines to help those studying photofacilitated membranes select or design photoactive molecules that will act as optimal carriers in liquid membranes under double illumination.

Facilitated transport in liquid membranes is a widely used separation method that has proven effective in removing a wide variety of solutes from mixtures.[1−6] A typical liquid membrane system involves feed and sweep phases separated by an immiscible solvent that constitutes the membrane. The feed phase usually contains a high concentration of a solute of interest as well as other solutes while the sweep phase has a negligible concentration of the solute of interest. The membrane solvent contains a high concentration of a carrier molecule that binds selectively and reversibly to the solute of interest as it enters the membrane at the feed interface. The solute itself has a low solubility in the membrane solvent so its unfacilitated diffusion rate is very low. The carrier−solute complex diffuses across the membrane to the sweep interface where the solute decomplexes from the carrier and diffuses into the sweep phase. In this way, the solute of interest is separated from the mixture in the feed solution with high selectivity. These types of facilitated liquid membranes rely on a high solute concentration gradient between the feed and sweep phases to maintain solute flux across the membrane in the desired direction. Theoretical studies of facilitated transport in liquid membranes have led to a greater understanding of the carrier and membrane properties that lead to optimal transport.[1]

The potential benefits of facilitated transport in liquid membranes can be extended by the use of a photoactive carrier to produce a photofacilitated liquid membrane.[7] In a photofacilitated liquid membrane, shown in Figure 1, the carrier (B) exists in two forms, depicted as B_s and B_w in the figure. B_s binds strongly to the solute of interest (denoted as A), while B_w binds weakly to A. When light of the appropriate wavelength to enhance the conversion of B_w to B_s impinges on the feed interface, the concentration of B_s increases allowing more complexation of the solute and enhanced solute uptake into the membrane. The strongly bound complex diffuses across the membrane to the sweep interface. The sweep interface is illuminated with light of the wavelength necessary to convert the strongly bound complex to the weakly bound complex. Note that the wavelengths of light impinging on each interface will be different. The weakly bound complex falls apart, resulting in a high concentration of free solute at the sweep interface and rapid flux of solute into the sweep phase. As a result of this process, called photomodulation, the overall flux of the solute is greatly enhanced over the flux in the dark.

The use of photofacilitated liquid membranes provides a number of advantages over traditional liquid membranes. Since flux in the light can be much greater than flux in the dark, transport can be switched on and off with light so that transport only occurs when desired. If light is focused on one part of the membrane, solute flux will be enhanced in that area, providing spatial control over transport. Since the carrier is specific for a particular solute in the feed solution, enhancing the total flux of that solute with light also enhances the selectivity of the membrane, providing control over selectivity.

A number of experimental and theoretical studies have explored singly illuminated photofacilitated liquid membranes in which only one side of the membrane is illuminated at a time.[8−24] In general, investigators have demonstrated that it is possible to obtain significantly higher solute flux under illumination than in the dark and that it is possible to control transport with light.[8−20] Theoretical studies in this area have provided information about what carrier and membrane properties will provide optimal conditions for photomodulation of solute transport.[21−23] These studies have indicated that membranes containing carriers that are primarily in the weakly binding form in the dark with the sweep side illuminated should show performance superior to that of membranes containing carriers that are predominantly in the strongly binding form in the dark with the feed side illuminated. Results of experiments

* Corresponding author. E-mail: Teresa_Longin@redlands.edu.

10.1021/jp053253t CCC: $30.25
Published on Web 10/18/2005

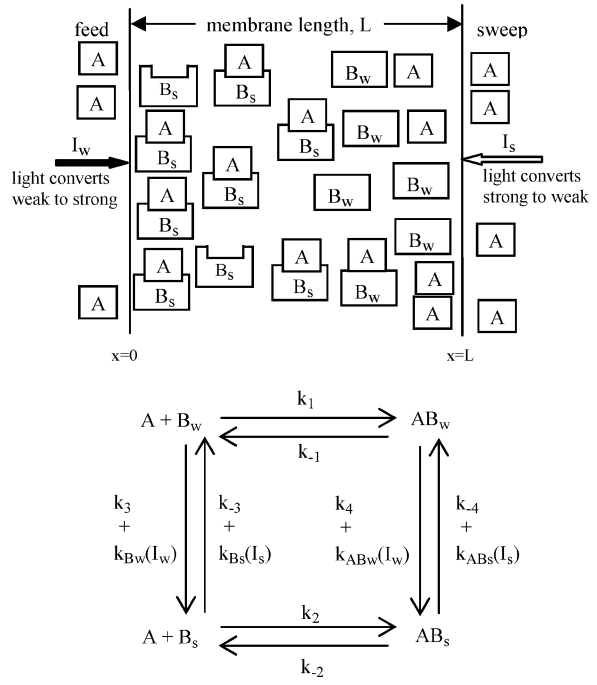

Figure 1. Schematic depiction of a doubly illuminated photofacilitated liquid membrane and the reaction scheme used as the model for photofacilitated transport in liquid membranes. The solute of interest is denoted as A, the weakly binding form of the carrier as B_w, and the strongly binding form of the carrier as B_s. The weakly bound form of the complex is denoted as AB_w and the strongly bound form of the complex as AB_s. The light impinging on the feed side of the membrane is of the proper wavelength to convert the weakly binding forms of the carrier and complex to the strongly binding form with a light intensity of I_w. The sweep side is illuminated with light of the correct wavelength to convert the strongly binding forms of the carrier and complex to the weakly binding forms at a light intensity of I_s. The wavelengths of light must be different on the two sides.

developed to test the predictions of the singly illuminated liquid membrane models show good agreement with the results predicted by the models[17] suggesting that the models for singly illuminated membranes are valid.

We have undertaken a theoretical study of a rarely investigated form of photomodulated membranes in which light (of different wavelengths) impinges on each side of the membrane simultaneously to produce a doubly illuminated liquid membrane[25] as shown in Figure 1. Many carriers used in experimental membranes and many potential carriers are photoactive in both the strongly and weakly binding forms[8−17,25−34] and so should be amenable to double illumination. We have simulated solute flux in the dark, under single illumination, and under double illumination for a range of carrier and membrane properties to determine which types of carriers would show significantly improved performance under double illumination relative to single illumination.

The Model

Our model for doubly illuminated liquid membranes depicted in Figure 1 is based on models developed for singly illuminated liquid membranes.[22−24] In the model for doubly illuminated liquid membranes, both the weakly and strongly binding forms of the carrier and complex are photoactive and light of the appropriate wavelength increases the rate of conversion from one form to the other. Not all carriers used in single illumination studies would be suitable candidates for doubly illuminated membranes, since they involve a carrier for which the photoexcited state is the weakly binding form and the weakly binding form cannot be converted to the strongly binding form with light.[7,18−20] However, a significant number of carriers used in single illumination studies as well as other potential carriers could be candidates for use in doubly illuminated liquid membranes.[8−17,25−34]

The solute is depicted as species A, the weakly binding form of the carrier as B_w, and the strongly binding form of the carrier as B_s. The carrier−solute complex can be in the strongly bound form, AB_s, or the weakly bound form, AB_w. The binding equilibria are defined in the following equations:

$$A + B_w \underset{k_{-1}}{\overset{k_1}{\rightleftharpoons}} AB_w \qquad K_w = \frac{k_1}{k_{-1}} \tag{1}$$

$$A + B_s \underset{k_{-2}}{\overset{k_2}{\rightleftharpoons}} AB_s \qquad K_s = \frac{k_2}{k_{-2}} \tag{2}$$

Since both the strongly and weakly binding forms of the carrier and the complex are photoactive, the rate constant for conversion between each form has a thermal component (present in both the dark and light), as well as a light intensity dependent component. The interconversion rate constants govern the equilibrium constants between the strongly and weakly binding forms of the carrier and complex. Consequently, the equilibrium constants will have a purely thermal "dark" component and a light intensity dependent component as shown in the following equations:

$$B_w \underset{k_{-3} + k_{B_s}(I_s)}{\overset{k_3 + k_{B_w}(I_w)}{\rightleftharpoons}} B_s \qquad K_{caro} = \frac{k_3}{k_{-3}} \tag{3}$$

$$K_{car}(I) = \frac{k_3 + k_{B_w}(I_w)}{k_{-3} + k_{B_s}(I_s)}$$

$$AB_w \underset{k_{-4} + k_{AB_s}(I_s)}{\overset{k_4 + k_{AB_w}(I_w)}{\rightleftharpoons}} AB_s \qquad K_{como} = \frac{k_4}{k_{-4}} \tag{4}$$

$$K_{com}(I) = \frac{k_4 + k_{AB_w}(I_w)}{k_{-4} + k_{AB_s}(I_s)}$$

In the above equations, I_w is defined as the light intensity at the wavelength that will convert the weakly binding forms to the strongly binding forms of the carrier and complex. I_s is defined as the light intensity at the wavelength needed to convert the strongly binding forms to the weakly binding forms of the carrier and complex. The subscripts car and com denote carriers and complexes, respectively. K_{caro} and K_{como} are equilibrium constants between the strongly and weakly binding forms of the carrier and complex forms under no illumination, while $K_{car}(I)$, and $K_{com}(I)$ are the light intensity dependent equilibrium constants. In this model the binding constants K_s and K_w are not directly affected by light. However, light does affect the relative concentrations of the strongly and weakly binding forms of the carrier and the complex. It is also assumed that the carrier excited state is short lived enough to not interfere in solute transport, unless the excited state is itself the weakly binding form of the carrier. None of the investigators exploring singly illuminated membrane transport who use carriers suitable for doubly illuminated membrane transport report concerns about interference from carrier excited states.[8−17]

Concentrations of the carrier and the complex are determined by reaction kinetics and by steady-state diffusion. Fick's second

law of diffusion provides the equations that describe the concentration profiles for each form of the carrier or complex at steady state.

$$\frac{d[A]}{dt} = 0 = -k_1[A][B_w] - k_2[A][B_s] + k_{-1}[AB_w] + k_{-2}[AB_s] + D_A\frac{d^2[A]}{dx^2} \quad (5)$$

$$\frac{d[B_w]}{dt} = 0 = -k_1[A][B_w] + k_{-1}[AB_w] - (k_3 + k_{B_w}(I_w))[B_w] + (k_{-3} + k_{B_s}(I_s))[B_s] + D_{B_w}\frac{d^2[B_w]}{dx^2} \quad (6)$$

$$\frac{d[B_s]}{dt} = 0 = -k_2[A][B_s] + k_{-2}[AB_s] + (k_3 + k_{B_w}(I_w))[B_w] - (k_{-3} + k_{B_s}(I_s))[B_s] + D_{B_s}\frac{d^2[B_s]}{dx^2} \quad (7)$$

$$\frac{d[AB_w]}{dt} = 0 = k_1[A][B_w] - k_{-1}[AB_w] - (k_4 + k_{AB_w}(I_w))[AB_w] + (k_{-4} + k_{AB_s}(I_s))[AB_s] + D_{AB_w}\frac{d^2[AB_w]}{dx^2} \quad (8)$$

$$\frac{d[AB_s]}{dt} = 0 = k_2[A][B_s] - k_{-2}[AB_s] + (k_4 + k_{AB_w}(I_w))[AB_w] - (k_{-4} + k_{AB_s}(I_s))[AB_s] + D_{AB_s}\frac{d^2[AB_s]}{dx^2} \quad (9)$$

The light intensity profiles are calculated using the Beer−Lambert law in its differential form.

$$\frac{dI_s}{dx} = I_s(\tilde{E}_{B_s}[B_s] + \tilde{E}_{AB_s}[AB_s]) \quad (10)$$

$$\frac{dI_w}{dx} = -I_w(\tilde{E}_{B_w}[B_w] + \tilde{E}_{AB_w}[AB_w]) \quad (11)$$

In these equations $\tilde{E}_{B_s}$ and $\tilde{E}_{AB_s}$ are the molar absorptivity coefficients for the strongly binding forms of the carrier and the carrier−solute complex, respectively. $\tilde{E}_{B_w}$ and $\tilde{E}_{AB_w}$ are the molar absorptivity coefficients for the weakly binding forms of the carrier and the carrier−solute complex, respectively. Practically, the complete separation of active wavelengths might be a challenge to achieve since many photoactive carriers are likely to have overlapping absorption spectra for the strongly and weakly binding forms. However, careful filtering can produce wavelengths that are exclusive to each form.

In the model, we assume that the carrier is much larger than the solute so that the carrier−solute complex is not significantly larger than the free carrier. Consequently, the diffusion coefficients of both forms of the carrier−solute complex (D_{AB}) are essentially the same as those of both forms of the free carrier. This assumption has been used in a number of previous theoretical studies of facilitated transport in liquid membranes[1,21,22,35] and applies to most of the carriers and solutes used in membrane transport studies cited in this paper. The total concentration of all forms of the carrier (free and complexed) will be constant across the membrane such that

$$C_T = [B_w] + [B_s] + [AB_w] + [AB_s] \quad (12)$$

C_T is the total concentration of carrier, both free and complexed, in the membrane. Boundary conditions for this membrane are as follows:

inside the membrane at the feed interface,

$$x = 0,\ [A] = [A]_o$$

$$\frac{d[B_w]}{dx} = \frac{d[B_s]}{dx} = \frac{d[AB_w]}{dx} = \frac{d[AB_s]}{dx} = 0 \quad (13)$$

$$I_w = I_{o,w}$$

inside the membrane at the sweep interface,

$$x = L,\ [A] = [A]_L = 0$$

$$\frac{d[B_w]}{dx} = \frac{d[B_s]}{dx} = \frac{d[AB_w]}{dx} = \frac{d[AB_s]}{dx} = 0 \quad (14)$$

$$I_s = I_{o,s}$$

Under these conditions, all forms of the carrier are nonvolatile and are confined within the membrane. These conditions also indicate that there is a constant source of A at the feed side ($x = 0$) and that as the solute is transferred across the membrane to the sweep side ($x = L$) it is removed to maintain an effective solute concentration of zero at the sweep interface. We assume that the feed side is illuminated at the appropriate wavelength of light to convert the weakly binding forms of the carrier and complex to the strongly binding forms. Conversely, at the sweep interface, the wavelength of light is chosen to convert the strongly binding forms of the carrier and complex to the weakly binding forms.

At steady state, the total flux of solute across the membrane is constant and described by Fick's first law of diffusion

$$J_A = -D_A\frac{d[A]}{dx} - D_{AB}\frac{d[AB_w]}{dx} - D_{AB}\frac{d[AB_s]}{dx} \quad (15)$$

Parameters were made dimensionless in order to apply this model to a wide variety of systems. Using our dimensionless parameters, rate constants can be separated out from the equilibrium constants, enabling separate assessments of thermodynamic and kinetic characteristics. Thus the carrier parameters for optimal transport can be determined. Parameters for a specific molecule can be compared to optimal parameters to determine if the molecule will make a reasonable carrier.

The concentration of the solute at every point in the membrane is normalized by dividing by the solute concentration inside the membrane at the feed interface, $[A]_o$. $[A]_o$ is not the same as the concentration of the solute in the bulk feed solution and will be controlled by the partition coefficient for the solute between the feed and sweep solvents. Typically, $[A]_o$ is several orders of magnitude lower than the solute concentration in the bulk feed phase. The concentrations of the carrier and the complex are normalized by dividing by the total concentration of the carrier, C_T. The dimensionless position of the solute in the membrane, χ, is defined by normalizing solute position x by the membrane length, L.

$$\bar{A} = \frac{[A]}{[A]_o}, \qquad \bar{B}_w = \frac{[B_w]}{C_T}, \qquad \bar{B}_s = \frac{[B_s]}{C_T}$$

$$\bar{A}\bar{B}_w = \frac{[AB_w]}{C_T}, \qquad \bar{A}\bar{B}_s = \frac{[AB_s]}{C_T} \tag{16}$$

$$\chi = \frac{x}{L}$$

The decomplexation rate constants are related to the diffusion coefficient that applies to all forms of the carrier and complex by

$$\epsilon_w = \frac{D_{AB}}{L^2 k_{-1}}, \qquad \epsilon_s = \frac{D_{AB}}{L^2 k_{-2}} \tag{17}$$

The above parameters relate the reaction times to diffusion times; small values of ϵ_w and ϵ_s indicate large rate constants and fast decomplexation reaction rates.

The binding equilibrium constants are made dimensionless by adjusting for the concentration of solute at the feed interface. Equilibrium constants that describe each form of the carrier and complex are shown below:

$$K_w^{\,d} = \frac{k_1}{k_{-1}}[A]_o, \qquad K_s^{\,d} = \frac{k_2}{k_{-2}}[A]_o$$

$$K_{caro} = \frac{k_3}{k_{-3}} = \frac{[B_s]}{[B_w]}, \qquad K_{como} = \frac{k_4}{k_{-4}} = \frac{[AB_s]}{[AB_w]} \tag{18}$$

The mobility parameter, α, relates the mobility of the carrier to the mobility of the solute.

$$\alpha = \frac{D_{AB} C_T}{D_A A_o} \tag{19}$$

The light intensities I_w and I_s are normalized by the respective incident light intensities $I_{o,w}$ and $I_{o,s}$:

$$\bar{I}_w = \frac{I_w}{I_{o,w}}, \qquad \bar{I}_s = \frac{I_s}{I_{o,s}} \tag{20}$$

The molar absorptivity coefficients for each form of the carrier and complex are rendered dimensionless as follows:

$$\beta_{car,w} = \tilde{E}_{B_w} C_T L, \qquad \beta_{car,s} = \tilde{E}_{B_s} C_T L \tag{21}$$

$$\beta_{com,w} = \tilde{E}_{AB_w} C_T L, \qquad \beta_{com,s} = \tilde{E}_{AB_s} C_T L \tag{22}$$

$\tilde{E}$ represents the molar absorptivity coefficient in units of L/mol cm.

The light intensity dependent rate constants are defined as simple linear functions of quantum yield for conversion, molar absorptivity coefficient, and incident light intensity.

$$k_{B_s}(I_s) = \Phi_{B_s} E_{B_s} I_{o,s} \tag{23}$$

$$k_{B_w}(I_w) = \Phi_{B_w} E_{B_w} I_{o,w} \tag{24}$$

$$k_{AB_s}(I_s) = \Phi_{AB_s} E_{AB_s} I_{o,s} \tag{25}$$

$$k_{AB_w}(I_w) = \Phi_{AB_w} E_{AB_w} I_{o,w} \tag{26}$$

In these equations Φ represents the quantum yield for conversion from one form of the carrier or complex to the other in units of moles converted/moles of photons absorbed. E represents the molar absorptivity coefficient in units of cm^2/mol.

The light intensities are introduced into the final dimensionless transport equations in the form of ratios of light-dependent rate constants to the thermal rate constants for interconversion between the forms of the carrier and complex. These ratios are denoted as η_{car} and η_{com}.

$$\eta_{car_s} = \frac{\Phi_{B_s} E_{B_s} I_{o,s}}{k_{-3}} \tag{27}$$

$$\eta_{car_w} = \frac{\Phi_{B_w} E_{B_w} I_{o,w}}{k_3} \tag{28}$$

$$\eta_{com_s} = \frac{\Phi_{AB_s} E_{AB_s} I_{o,s}}{k_{-4}} \tag{29}$$

$$\eta_{com_w} = \frac{\Phi_{AB_w} E_{AB_w} I_{o,w}}{k_4} \tag{30}$$

We also define a set of dimensionless parameters that relate reaction time for conversion between forms to diffusion time of the carrier or complex. We have chosen to call these parameters ϵ_{car} and ϵ_{com}, and they are defined in terms of $k_{-3} + k_{B_s}(I_s)$ and $k_{-4} + k_{AB_s}(I_s)$ to make the subscript notation consistent with ϵ_s and ϵ_w. The equations for the light intensity dependent ϵ values and equilibrium constants are as follows:

$$\epsilon_{car}(I) = \frac{D_{AB}}{L^2(k_{-3} + k_{B_s}(I_s))} = \frac{\epsilon_{caro}}{1 + \eta_{car,s}\bar{I}_s} \tag{31}$$

where $\epsilon_{caro} = D_{AB}/L^2 k_{-3}$

$$\epsilon_{com}(I) = \frac{D_{AB}}{L^2(k_{-4} + k_{AB_s}(I_s))} = \frac{\epsilon_{como}}{1 + \eta_{com,s}\bar{I}_s} \tag{32}$$

where $\epsilon_{como} = D_{AB}/L^2 k_{-4}$

$$K_{car}(I) = \frac{k_3 + k_{B_w}(I_w)}{k_{-3} + k_{B_s}(I_s)} = K_{caro}\left(\frac{1 + \eta_{car,w}\bar{I}_w}{1 + \eta_{car,s}\bar{I}_s}\right) \tag{33}$$

$$K_{com}(I) = \frac{k_4 + k_{AB_w}(I_w)}{k_{-4} + k_{AB_s}(I_s)} = K_{como}\left(\frac{1 + \eta_{com,w}\bar{I}_w}{1 + \eta_{com,s}\bar{I}_s}\right) \tag{34}$$

The resulting dimensionless, steady-state equations are

$$\frac{d^2\bar{A}}{d\chi^2} = \frac{\alpha K_w^{\,d}}{\epsilon_w}\bar{A}^*\bar{B}_w - \frac{\alpha}{\epsilon_w}\bar{A}\bar{B}_w + \frac{\alpha K_s^{\,d}}{\epsilon_s}\bar{A}^*\bar{B}_s - \frac{\alpha}{\epsilon_s}\bar{A}\bar{B}_s \tag{35}$$

$$\frac{d^2\bar{B}_w}{d\chi^2} = \frac{K_w^{\,d}}{\epsilon_w}\bar{A}^*\bar{B}_w - \frac{\bar{A}\bar{B}_w}{\epsilon_w} + \frac{K_{caro}}{\epsilon_{car_o}}(1 + \eta_{car_w}\bar{I}_w)\bar{B}_w - \frac{(1 + \eta_{car_s}\bar{I}_s)\bar{B}_s}{\epsilon_{caro}} \tag{36}$$

$$\frac{d^2\bar{B}_s}{d\chi^2} = \frac{K_s^{\,d}}{\epsilon_s}\bar{A}^*\bar{B}_s - \frac{\bar{A}\bar{B}_s}{\epsilon_s} - \frac{K_{caro}}{\epsilon_{caro}}(1 + \eta_{car_w}\bar{I}_w)\bar{B}_w + \frac{(1 + \eta_{car_s}\bar{I}_s)}{\epsilon_{caro}}\bar{B}_s \tag{37}$$

$$\frac{d^2\bar{A}\bar{B}_w}{d\chi^2} = \frac{-K_w^{\,d}}{\epsilon_w}\bar{A}^*\bar{B}_w + \frac{\bar{A}\bar{B}_w}{\epsilon_w} + \frac{K_{como}}{\epsilon_{como}}(1+\eta_{com_w}\bar{I}_w)\bar{A}\bar{B}_w - \frac{(1+\eta_{com_s}\bar{I}_s)}{\epsilon_{como}}\bar{A}\bar{B}_s \quad (38)$$

$$\frac{d^2\bar{A}\bar{B}_s}{d\chi^2} = \frac{-K_s^{\,d}}{\epsilon_s}\bar{A}^*\bar{B}_s + \frac{\bar{A}\bar{B}_s}{\epsilon_s} - \frac{K_{como}}{\epsilon_{como}}(1+\eta_{com_w}\bar{I}_w)\bar{A}\bar{B}_w + \frac{(1+\eta_{com_s}\bar{I}_s)}{\epsilon_{como}}\bar{A}\bar{B}_s \quad (39)$$

$$\frac{d\bar{I}_w}{d\chi} = \bar{I}_w(\beta_{car_w}\bar{B}_w + \beta_{com_w}\bar{A}\bar{B}_w) \quad (40)$$

$$\frac{d\bar{I}_s}{d\chi} = \bar{I}_s(\beta_{car_s}\bar{B}_s + \beta_{com_s}\bar{A}\bar{B}_s) \quad (41)$$

The dimensionless boundary conditions become:

at $\chi = 0$, $\bar{A} = 1$

$$\frac{d\bar{B}_w}{d\chi} = \frac{d\bar{B}_s}{d\chi} = \frac{d\bar{A}\bar{B}_w}{d\chi} = \frac{d\bar{A}\bar{B}_s}{d\chi} = 0$$

$$\bar{I}_{o,w} = 1 \quad (42)$$

at $\chi = 1$, $\bar{A} = \bar{A}_1$

$$\frac{d\bar{B}_w}{d\chi} = \frac{d\bar{B}_s}{d\chi} = \frac{d\bar{A}\bar{B}_w}{d\chi} = \frac{d\bar{A}\bar{B}_s}{d\chi} = 0$$

$$\bar{I}_{o,s} = 1 \quad (43)$$

The dimensionless mass balance equation on the carrier becomes

$$1 = \bar{B}_w + \bar{B}_s + \bar{A}\bar{B}_w + \bar{A}\bar{B}_s \quad (44)$$

The total dimensionless flux of solute is defined as follows:

$$N_{\bar{A}} = -\frac{d\bar{A}}{d\chi} - \alpha\frac{d\bar{A}\bar{B}_w}{d\chi} - \alpha\frac{d\bar{A}\bar{B}_s}{d\chi} \quad (45)$$

Other important parameters to characterize are the facilitation factors F' and F'':

$$F' = \frac{N_{\bar{A},light}}{N_{\bar{A},dark}} \quad (46)$$

$$F'' = \frac{N_{\bar{A},double,optimal}}{N_{\bar{A},single,optimal}} \quad (47)$$

F' is defined as the ratio of the highest total dimensionless flux of A under single or double illumination to the total dimensionless flux of A under no illumination. F'' is defined as the ratio of the maximum total dimensionless flux of A under double illumination to the maximum total dimensionless flux of A under single illumination.

Simulation Methodology. To simulate solute transport in liquid membranes, solutions must be found for the mass transport and light intensity equations. It is only necessary to solve three of the four dimensionless mass transport equations for the various forms of the carrier since the mass balance on the carrier can be used to calculate the fourth. Equations 35, 36, 37, and 39 were solved and eq 44 was used to determine $\bar{A}\bar{B}_w$. The FORTRAN program BVPFD (from the IMSL library) was used to obtain solutions.

To solve the mass transport equations, $K_w^{\,d}$, $K_s^{\,d}$, and $K_{car}(I)$ were defined and $K_{com}(I)$ was calculated as

$$K_{com}(I) = \frac{K_{car}(I)K_s^{\,d}}{K_w^{\,d}} \quad (48)$$

In addition, each η term is related to the other through ϵ_{car_o}, ϵ_{como}, β_{car}, and β_{com}. When solving the equations, η_{car_s}, η_{car_w}, $\beta_{car,s}$, $\beta_{car,w}$, $\beta_{com,s}$, and $\beta_{com,w}$ were defined and η_{com_s} and η_{com_w} were calculated as

$$\eta_{com_s} = \frac{\Phi_{AB_s}\eta_{car_s}\epsilon_{como}\beta_{com,s}}{\Phi_{B_s}\epsilon_{caro}\beta_{car,s}} \quad (49)$$

$$\eta_{com_w} = \frac{\Phi_{AB_w}\eta_{car_w}\epsilon_{como}\beta_{com,w}}{\Phi_{B_{ws}}\epsilon_{caro}\beta_{car,w}} \quad (50)$$

Throughout the calculations, the quantum yields were set to 1 since many potential carriers have high quantum yields for conversion. However, if the quantum yields for conversion for a potential carrier of interest are much less than 1, then the incident light intensity necessary to achieve a certain effect at a given value of η will be proportionally greater.

The program BVPFD allows the use of a logarithmic χ grid, providing points very close together at the edges of the membrane where the concentrations change rapidly and further apart toward the center of the membrane where the concentrations do not change as rapidly. If necessary, the program will automatically add more χ points in order to achieve convergence. For the series of simulations described in this paper, the number of χ points used for the initial guess was 201.

The dimensionless flux values obtained indicate how well the carrier transports the solute across the membrane with higher flux values indicating better transport. For the simulations done in these experiments, a given variable was changed and the rest were held constant to determine the light intensities which resulted in the highest flux values. For example, ϵ_{caro} and ϵ_{como} were changed systematically while $K_s^{\,d}$, $K_w^{\,d}$, β, α, K_{caro}, and K_{como} were kept constant. Simulations at each value of ϵ_{caro} and ϵ_{como} were run to determine the optimal fluxes under single and double illumination.

For each set of carrier properties, the first simulation run was with no light intensity on either side of the membrane to provide the inherent flux in the dark. To provide the optimal flux under single illumination, the light intensity was gradually increased on either the sweep side (for carriers with $K_{car} > 1$) or the feed side (for carriers with $K_{car} < 1$) until a maximum solute flux was obtained. Then the light intensity at the opposite interface was gradually increased until a maximum solute flux was again seen. This process was repeated until the increase in flux value with increase in light intensity began to level off, such that large increases in light intensity produced relatively small increases in flux value. The value at which the solute flux levels off is called the "maximum flux" for double illumination, even though the flux will continue to increase slightly with increases in light intensity.

The program results in the dark and under single illumination were compared to results obtained from previous models.[1,22,23] Results in the dark were identical to those obtained in modeling studies of liquid membranes operating under purely thermal conditions.[1] Results under single illumination were also identical

to those obtained for the models of singly illuminated liquid membranes.[23,24] The program does require a good initial guess when gradients at the interfaces are steep. Initial guesses for dark conditions and low light intensity were based on results for simulations of facilitated transport under purely thermal conditions.[1] As the light intensity was increased, results from lower light intensity solutions were used as initial guesses. Different initial guesses resulted in the same solution for a given set of parameter values.

The flux values, F' and F'', were plotted against values of the parameter being studied to determine trends in membrane performance as a function of carrier and membrane properties. These results can be used to determine what values of carrier and membrane properties are optimal for transport. This will help in determining what carriers will be appropriate for transport.

Results and Discussion

To investigate the benefits of double illumination over single illumination, we chose to separate the simulations into two parts. Realistically, a potential carrier will predominantly be in the strongly binding form in the dark, predominantly in the weakly binding form in the dark, or will have an equal concentration of the two forms. We first explored simulated transport for carriers that predominately exist as the strongly binding form in the dark ($[B_s]/[B_w] > 1$) and then looked at the case in which the carrier is predominantly in the weakly binding form in the dark ($[B_s]/[B_w] < 1$). The central focus of these investigations was to determine whether double illumination provided better transport of the solute across the membrane than single illumination and what carrier and membrane properties would make double illumination of the membrane beneficial.

Section 1: Carriers That Are Predominantly in the Strongly Binding Form in the Dark. In this case, simulations for single illumination initially were run with light impinging only on the sweep interface to turn the strongly binding forms of the carrier and complex to the weakly binding forms. After the maximum flux under single illumination was determined, the light intensity on the feed interface was increased to convert the weakly binding forms of the carrier and complex to the strongly binding forms and then the flux was optimized as described in the Simulation Methodology section.

Effect of ϵ_{caro} and ϵ_{como}. The variables ϵ_{caro} and ϵ_{como} (described by eqs 31 and 32) are dimensionless kinetic parameters that relate the reaction time for the interconversion between the strongly and weakly binding forms of the carrier and complex to diffusion time. Since ϵ_{caro} and ϵ_{como} are inversely proportional to the rate constants k_{-3} and k_{-4}, respectively, an increase in ϵ_{caro} and ϵ_{como} means a decrease in the rate constants for the conversion of the strongly binding forms to the weakly binding forms of the carrier and complex.

Increasing the light intensities increases the rates of interconversion between forms. This in turn results in an increase in the flux when one side of the membrane is illuminated. The flux increases even more as the membrane is doubly illuminated. Parts a and b of Figure 2 show that flux and F' fall off under single illumination with slow interconversion kinetics (meaning large ϵ_{caro} and ϵ_{como} values). However, under double illumination, the values obtained for flux and F' remain high and fairly constant even as the interconversion kinetics slow. As ϵ_{caro} and ϵ_{como} increase from 0.1 to 100, it appears that double illumination overcomes the slow kinetics represented by the large ϵ_{caro} and ϵ_{como} values, resulting in high values of F'' as shown in Figure 2c.

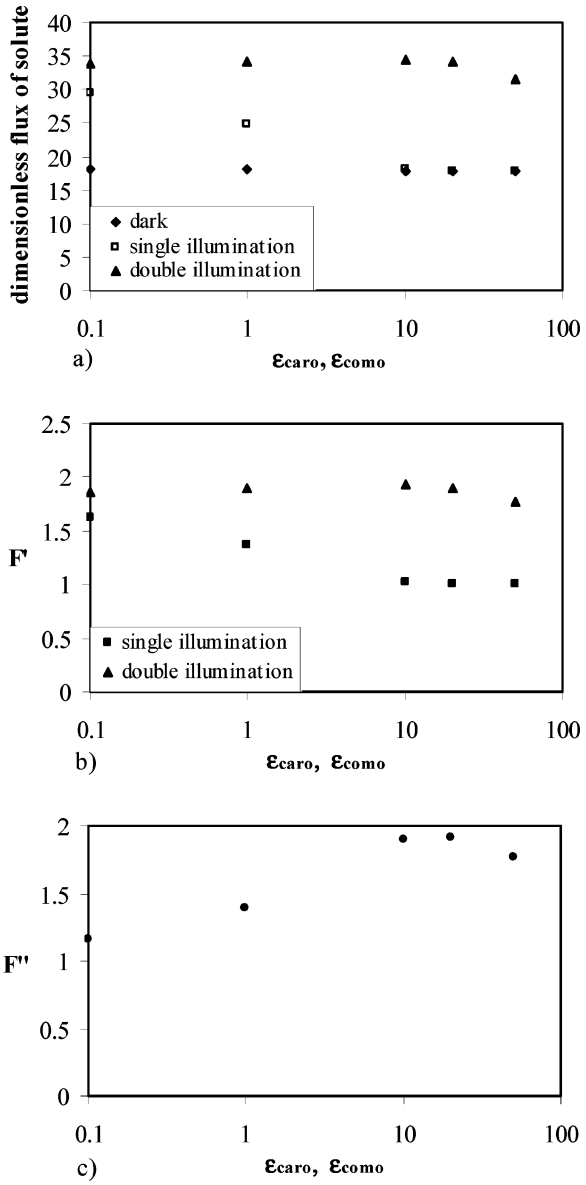

Figure 2. Plots of dimensionless flux of solute in the dark and under illumination, F' under double and single illumination, and F'' versus ϵ_{caro} and ϵ_{como} for carriers that are predominantly in the strongly binding form in the dark. For all cases, $K_s^d = 10$, $K_w^d = 0.1$, $K_{caro} = 10$, $K_{como} = 1000$, $\alpha = 50$, $\beta_{car,w} = \beta_{car,s} = \beta_{com,w} = \beta_{com,s} = 10$, and $\epsilon_s = \epsilon_w = 0.01$. (a) Plots of the dimensionless flux of solute versus ϵ_{caro} and ϵ_{como} in the dark, under single illumination, and under double illumination. (b) Plots of the degree of photomodulation, F', versus ϵ_{caro} and ϵ_{como} under single and double illumination. (c) Plot of the ratio of maximum solute flux under double illumination to the maximum solute flux under single illumination, F'', versus ϵ_{caro} and ϵ_{como}.

This result can be explained by the solute concentration in the membrane. Parts a and b of Figure 3 show the normalized concentration of the solute across the membrane for ϵ_{caro} and ϵ_{como} at values of 20 and 1, respectively. The value of normalized [A] at $\chi = 0$ represents the normalized solute concentration in the membrane at the feed interface while the value at $\chi = 1$ represents normalized solute concentration in the membrane at the sweep interface. Under single illumination at ϵ_{caro} and ϵ_{como} values of 20, solute concentration within the membrane is fairly low and the concentration gradients at the edges are not steep, as shown in Figure 3a. Since Fick's first law of diffusion defines flux as being proportional to the change in concentration over distance (see eqs 15 and 45), the low concentration gradients at the edges represent low flux. In contrast, Figure 3b shows

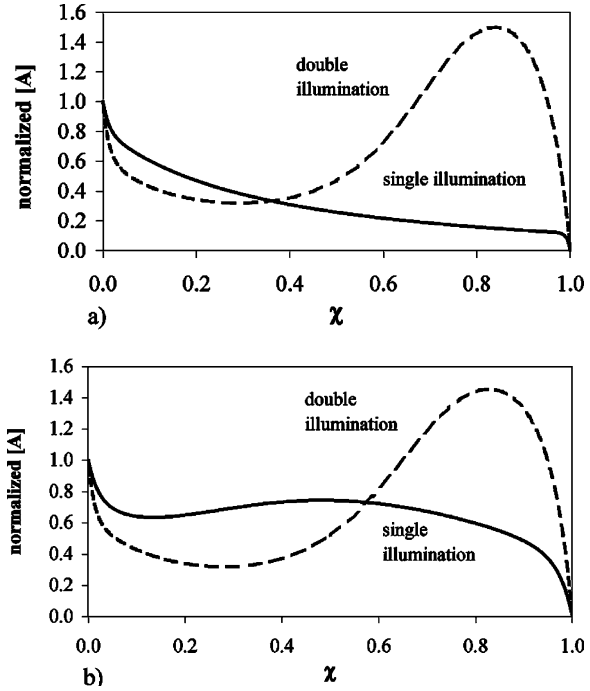

Figure 3. Normalized solute concentration profiles across a membrane in which the carrier is predominantly in the strongly binding form in the dark. For this membrane, $K_s^d = 10$, $K_w^d = 0.1$, $K_{caro} = 10$, $K_{como} = 1000$, $\alpha = 50$, $\beta_{car,w} = \beta_{car,s} = \beta_{com,w} = \beta_{com,s} = 10$, and $\epsilon_s = \epsilon_w = 0.01$. (a) Normalized solute concentration versus normalized membrane length, χ, for $\epsilon_{caro} = \epsilon_{como} = 20$, which represents relatively small interconversion rate constants. (b) Normalized solute concentration versus normalized membrane length, χ, for $\epsilon_{caro} = \epsilon_{como} = 1$, which represents moderate interconversion rate constants.

that for ϵ_{caro} and ϵ_{como} values of 1 under single illumination, solute concentration within the membrane is high and the concentration gradients at the edges are steep, representing rapid transport. Under double illumination, solute concentrations within the membrane are high at both 20 and 1, and the concentration gradients at the edges are steep, representing rapid transport. Indeed under double illumination, the solute concentration profiles for ϵ_{caro} and ϵ_{como} of 20 and ϵ_{caro} and ϵ_{como} of 1 are the same.

We chose to use ϵ_{caro} and ϵ_{como} values of 1 for further simulations in which we varied other parameters. At these values, flux and photomodulation factors under both single and double illumination are high, while double illumination clearly is beneficial.

Effects of K_s^d and K_w^d. K_s^d denotes the binding constant for the strongly binding form of the carrier and is defined in eq 18. K_w^d is the binding equilibrium constant for the weakly binding form of the carrier and is also defined in eq 18. Determining the optimal value of these factors separately is a bit tricky. Keeping the value of K_w^d constant and varying K_s^d means that the ratio between the two varies, which will have an impact on flux. Maintaining a constant ratio between K_s^d and K_w^d while varying K_s^d means that K_w^d must also be varied. We chose to vary K_s^d while keeping the ratio of K_s^d to K_w^d constant to determine the optimal value of K_s^d. We then varied the value of K_w^d, keeping the value of K_s^d constant to determine optimal values of K_w^d and optimal ratios of K_s^d to K_w^d.

We varied K_s^d between 100 and 1, while varying the value of K_w^d between 1 and 0.01, keeping the ratio of K_s^d to K_w^d constant at 100. Figure 4a shows that solute flux gradually increases, peaks, and then slowly decreases with increasing K_s^d under all illumination conditions. However, flux under

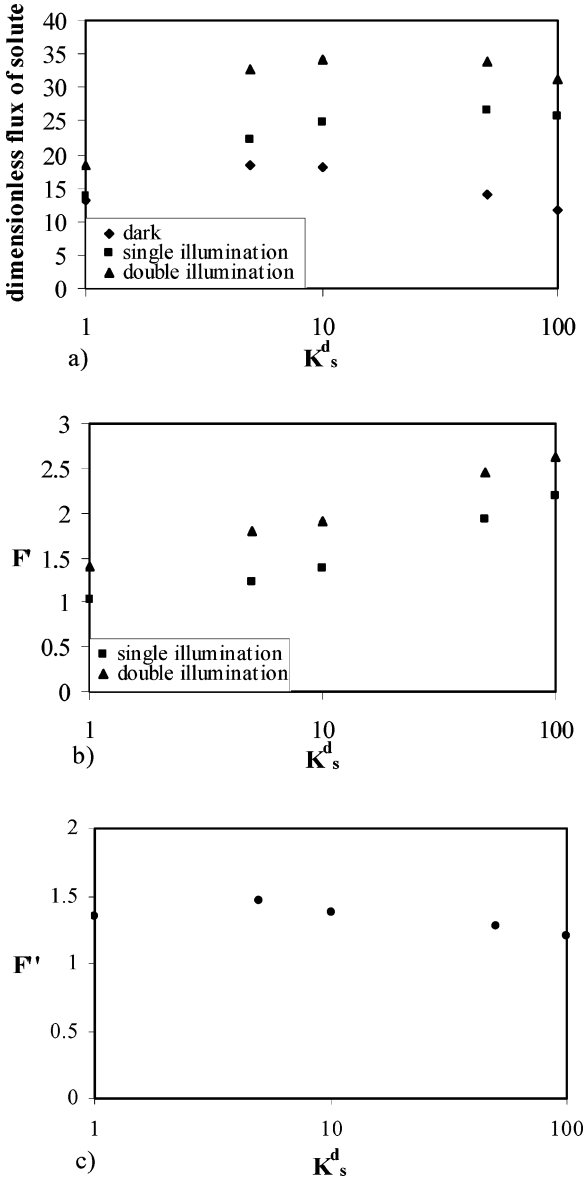

Figure 4. Plots of dimensionless flux of solute in the dark and under illumination, F' under double and single illumination, and F'' versus K_s^d for carriers that are predominantly in the strongly binding form in the dark. For all cases, $K_{caro} = 10$, $K_{como} = 1000$, $\alpha = 50$, $\beta_{car,w} = \beta_{car,s} = \beta_{com,w} = \beta_{com,s} = 10$, $\epsilon_{caro} = \epsilon_{como} = 1.0$, and $\epsilon_s = \epsilon_w = 0.01$. The ratio of K_s^d/K_w^d is held constant at 100. (a) Plots of the dimensionless flux of solute versus K_s^d in the dark, under single illumination, and under double illumination. (b) Plots of the degree of photomodulation, F', versus K_s^d under single and double illumination. (c) Plot of the ratio of maximum solute flux under double illumination to the maximum solute flux under single illumination, F'', versus K_s^d.

illumination is much higher than dark flux at higher values of K_s^d, so F' increases with increasing K_s^d under single and double illumination as shown in Figure 4b. The increase in solute flux with increasing K_s^d is much greater under single illumination than under double illumination, so F'' decreases with increasing K_s^d (Figure 4c). It appears that a moderate K_s^d is optimal for maximum benefits of double illumination while still providing good results for single illumination. Since we are interested in determining the conditions for which double illumination is beneficial while still providing for good overall membrane performance, we chose to perform further simulations at $K_s^d = 10$.

Keeping K_s^d at 10, we varied K_w^d to determine how the value of the weak binding constant affects transport. As can

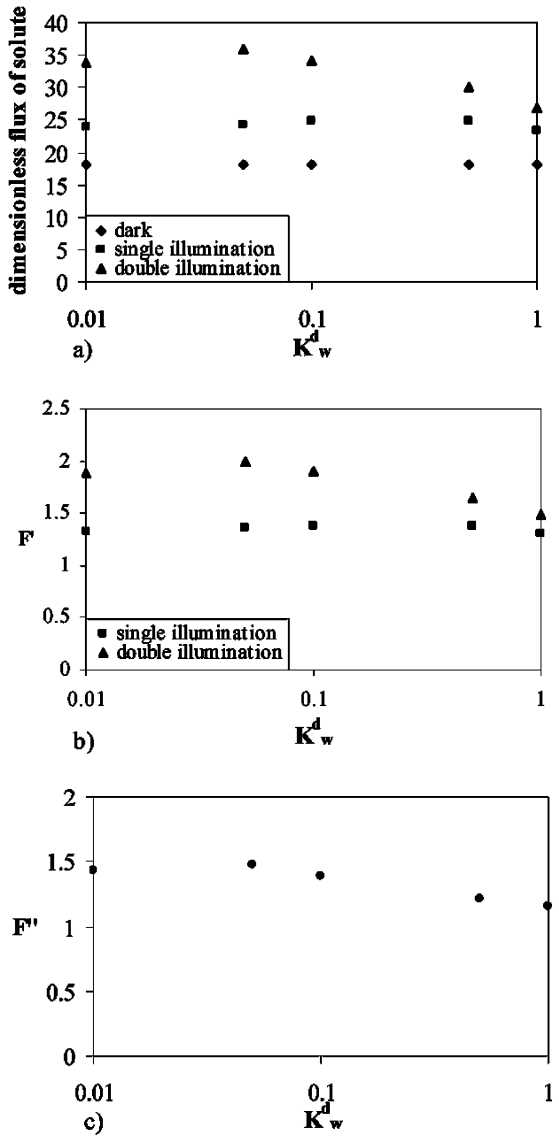

Figure 5. Plots of dimensionless flux of solute in the dark and under illumination, F' under double and single illumination, and F'' versus K_w^d for carriers that are predominantly in the strongly binding form in the dark. For all cases, $K_s^d = 10$, $K_{caro} = 10$, $\alpha = 50$, $\beta_{car,w} = \beta_{car,s} = \beta_{com,w} = \beta_{com,s} = 10$, $\epsilon_{caro} = \epsilon_{como} = 1.0$, and $\epsilon_s = \epsilon_w = 0.01$. (a) Plots of the dimensionless flux of solute versus K_w^d in the dark, under single illumination, and under double illumination. (b) Plots of the degree of photomodulation, F', versus K_w^d under single and double illumination. (c) Plot of the ratio of maximum solute flux under double illumination to the maximum solute flux under single illumination, F'', versus K_w^d.

be seen in parts a and b of Figure 5, the dimensionless flux and F' under single illumination are almost unaffected by changing K_w^d. However, under double illumination, transport improves upon decreasing K_w^d from 1.0 to 0.1 and then appears to stay fairly constant for smaller values of K_w^d. Consequently, F'' also increases and then levels off as K_w^d decreases, as seen in Figure 5c.

The trend for the single illumination values as a function of K_w^d is markedly different for faster interconversion kinetics. The results in Figure 5 are from simulations run with ϵ_{caro} and ϵ_{como} both equal to 1.0, which represents moderate rate constants for interconversion between the strongly and weakly binding forms of the carrier. For smaller values of ϵ_{caro} and ϵ_{como} (meaning larger interconversion rate constants), both dimensionless flux and F' under single illumination increase as the value of K_w^d decreases. This is consistent with results from work on photomodulation under single illumination only.[22,23] While solute flux and F′ values under double illumination are greater than the flux and F' under single illumination, the difference is rather small. In contrast, for smaller interconversion rate constants, the performance under double illumination is significantly greater than that under single illumination.

Consequently, for carriers with fast interconversion kinetics, K_w^d should be small (at least 100 times smaller than K_s^d), and double illumination will provide only a small improvement in performance over single illumination. For carriers with slow interconversion kinetics, K_w^d should be small and double illumination can be expected to provide significantly better transport than single illumination. We chose to use K_s^d equal to 10 and K_w^d equal to 0.1 to test the effects of other parameters.

Effects of K_{caro} and K_{como}. K_{caro} is the equilibrium constant that describes the concentration ratio between the strongly binding and weakly binding forms of the carrier in the dark, and K_{como} is the equilibrium constant between the two forms of the complex in the dark as defined in eq 18. When the membrane is illuminated, these equilibrium constants become light intensity dependent, as described in eqs 3 and 4. In the test of these parameters, the value of K_{caro} was defined and K_{como} was determined by eq 48, as described in the Simulation Methodology section.

Parts a and b of Figure 6 show that both flux and F' increase with increasing K_{caro} under single illumination. Under double illumination, dimensionless flux and F' increase and then level off as K_{caro} increases. Consequently, F'' actually decreases with increasing K_{caro}, as shown in Figure 6c. Since a K_{caro} of 10 provided good overall membrane performance and gave better transport under double illumination, that value was used for further simulations.

Effects of α. The parameter α relates the mobility of the carrier to the mobility of the solute and is described by eq 19. As α increases, the concentration of carrier relative to the concentration of solute increases and more solute is drawn into the membrane. Parts a and b of Figure 7 show that as α increases, the flux and F' also increase for both single and double illumination. Since α is the mobility of the carrier relative to the mobility of the solute, we expect to see higher flux and a higher F' as α is increased. These results are consistent with previous modeling studies involving singly illuminated photofacilitated membranes.[22,23] The increase in transport with α is greater under double illumination than under single illumination for slow carrier interconversion kinetics (large values of ϵ_{caro} and ϵ_{como}), so that F'' also increases with α (Figure 7c).

For faster carrier interconversion kinetics, the difference between double and single illumination is much smaller. This phenomenon is due to differences in carrier concentrations at optimal light intensities for different values of carrier interconversion rate constants. For fast carrier interconversion kinetics, the optimal light intensity for both single and double illumination results in a very low concentration of the strongly binding form of the carrier at the sweep interface as shown in Figure 8a. This results in a large amount of free solute and high flux.

In contrast, for slow interconversion kinetics, the optimal light intensity for single illumination is lower, leaving a significant amount of the strongly binding form of the carrier at the sweep interface, as shown in Figure 8b. Higher light intensities reduce the concentration of the strongly binding form of the carrier at the sweep interface, but because the interconversion kinetics are slow, this results in overall depletion of the strongly binding form of the complex throughout the membrane. This in turn results in a lower solute flux because less solute is drawn into

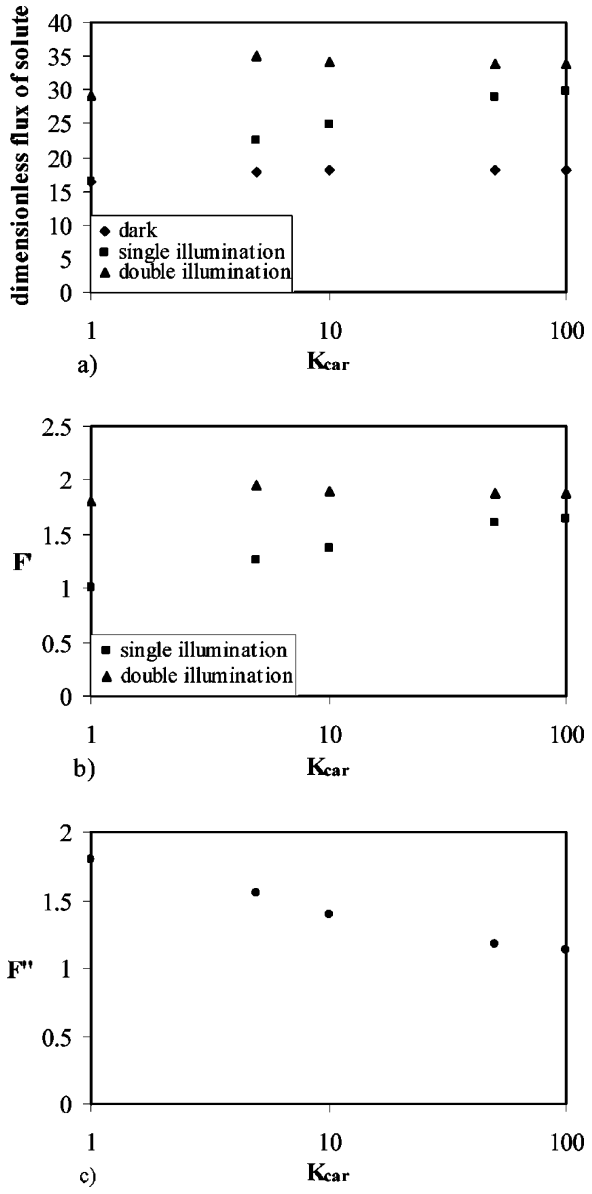

Figure 6. Plots of dimensionless flux of solute in the dark and under illumination, F' under double and single illumination, and F'' versus K_{caro} for carriers that are predominantly in the strongly binding form in the dark. For all cases, $K_s^d = 10$, $K_w^d = 0.1$, $\alpha = 50$, $\beta_{car,w} = \beta_{car,s} = \beta_{com,w} = \beta_{com,s} = 10$, $\epsilon_{caro} = \epsilon_{como} = 1.0$, and $\epsilon_s = \epsilon_w = 0.01$. (a) Plots of the dimensionless flux of solute versus K_{caro} in the dark, under single illumination, and under double illumination. (b) Plots of the degree of photomodulation, F', versus K_{caro} under single and double illumination. (c) Plot of the ratio of maximum solute flux under double illumination to the maximum solute flux under single illumination, F'', versus K_{caro}.

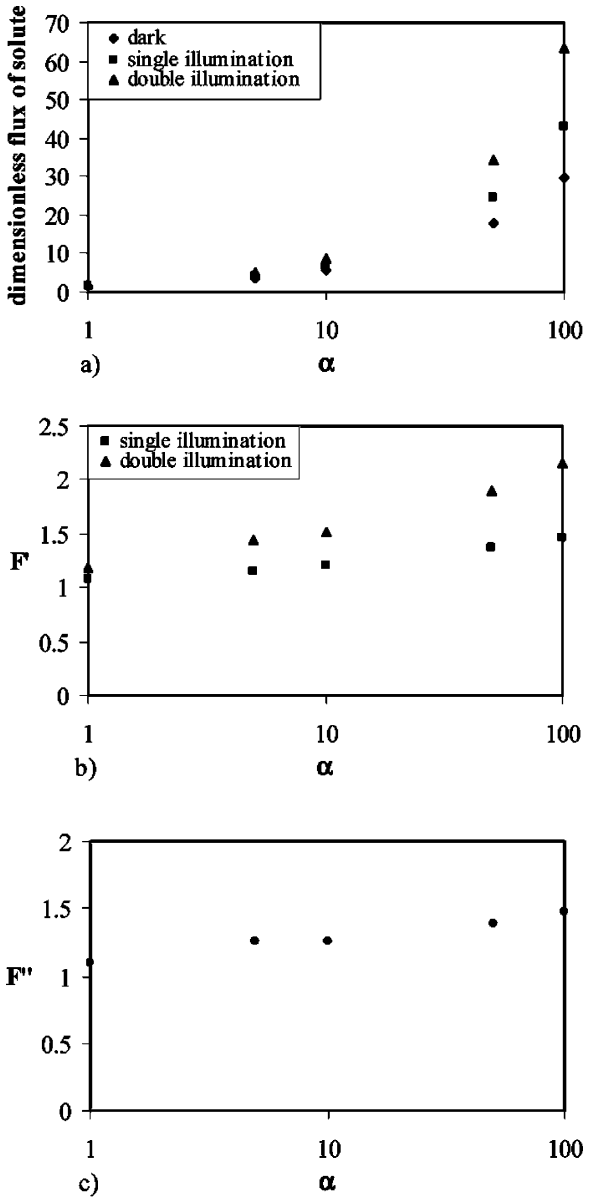

Figure 7. Plots of dimensionless flux of solute in the dark and under illumination, F' under double and single illumination, and F'' versus α for carriers that are predominantly in the strongly binding form in the dark. For all cases, $K_s^d = 10$, $K_w^d = 0.1$, $K_{caro} = 10$, $K_{como} = 1000$, $\beta_{car,w} = \beta_{car,s} = \beta_{com,w} = \beta_{com,s} = 10$, $\epsilon_{caro} = \epsilon_{como} = 1.0$, and $\epsilon_s = \epsilon_w = 0.01$. (a) Plots of the dimensionless flux of solute versus α in the dark, under single illumination, and under double illumination. (b) Plots of the degree of photomodulation, F', versus α under single and double illumination. (c) Plot of the ratio of maximum solute flux under double illumination to the maximum solute flux under single illumination, F'', versus α.

the membrane. Conversely, under double illumination at optimal light intensity, the concentration of the strongly binding form of the carrier is driven very low at the sweep interface as shown in Figure 8b. The overall concentration of the strongly binding form is not depleted because the weakly binding form is rapidly converted back to the strongly binding form at the illuminated feed interface. Thus, double illumination provides greater benefits for membranes containing carriers with slow interconversion kinetics.

At low values of α, the concentration of carrier is not much greater than that of the solute. Consequently, the solute itself begins to have an impact on the ratio between the strongly and weakly binding forms of the carrier due to the binding equilibrium constants, and the difference between the performance under single and double illumination lowers regardless of interconversion kinetics. Consequently, values of α greater than 10 are required for good membrane performance under both single and double illumination.

Effects of β. The term β is the normalized molar absorptivity coefficient for the photoactive form of the carrier or the complex and is defined by eqs 21 and 22. While there are four different independent β terms ($\beta_{car,s}$, $\beta_{car,w}$, $\beta_{com,s}$, and $\beta_{com,w}$), for simplicity's sake we have chosen to set them all equal to each other to explore trends in membrane performance as a function of β.

Figure 9a shows that the solute flux increases as β increases for both doubly and singly illuminated membranes. However,

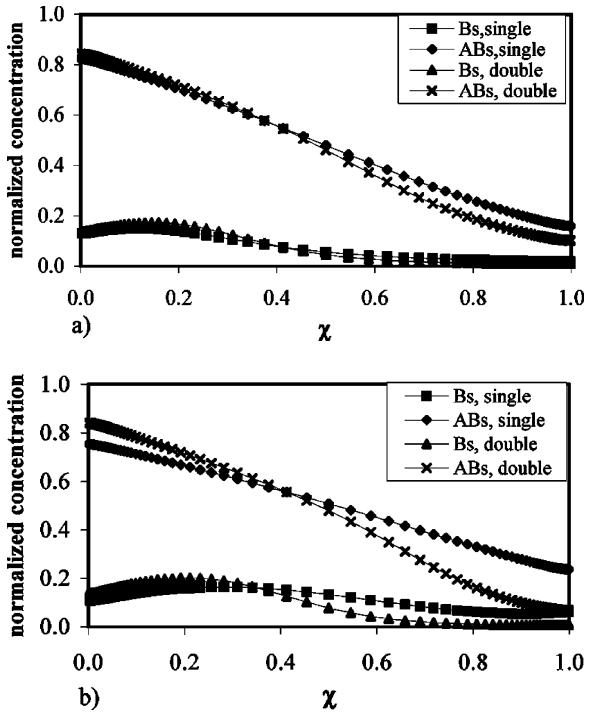

Figure 8. Profiles of the normalized concentrations of the strongly binding forms of the carrier and complex across the membrane under double and single illumination. For this membrane, the carrier is predominantly in the strongly binding form in the dark. For all cases, $K_s^d = 10$, $K_w^d = 0.1$, $K_{caro} = 10$, $K_{como} = 1000$, $\beta_{car,w} = \beta_{car,s} = \beta_{com,w} = \beta_{com,s} = 10$, and $\epsilon_s = \epsilon_w = 0.01$. (a) Normalized concentrations of the strongly binding forms of the carrier and complex versus normalized membrane length, χ, under double and single illumination. For this case, $\epsilon_{caro} = \epsilon_{como} = 0.01$, which represents large interconversion rate constants. (b) Normalized concentrations of the strongly binding forms of the carrier and complex versus normalized membrane length, χ, under double and single illumination. For this case, $\epsilon_{caro} = \epsilon_{como} = 1.0$, which represents moderate interconversion rate constants.

at high values of β the flux and F' under double illumination level off, while the flux and F' under single illumination continue to increase as shown in parts a and b of Figure 9. Consequently, F'' decreases at high values of β as shown in Figure 9c. Thus a moderate β (between 10 and 50) is desirable to have a large benefit from double illumination.

Effects of ϵ_s and ϵ_w. ϵ_s and ϵ_w are related to the decomplexation rate constants. These parameters control the rate at which the solute is released from the complex and are defined by eq 17. Since ϵ_s and ϵ_w are inversely proportional to the rate constants for decomplexation, high values of ϵ_s and ϵ_w mean small decomplexation rate constants. Fast decomplexation kinetics (meaning small values of ϵ_s and ϵ_w) are needed for good membrane performance, as demonstrated in theoretical papers on membranes containing nonphotoactive carriers and on singly illuminated membranes.[1,22−24]

As ϵ_s and ϵ_w are increased from 0.01 to 100, the flux, F', and F'' all decrease. Double illumination does not compensate for the decrease in the rate of release of the solute. These results are consistent with prior modeling studies of facilitated transport in liquid membranes.[1,22−24] Consequently, for optimal membrane performance, ϵ_s and ϵ_w should be small (<1).

Section 2: Carriers That Are Predominantly in the Weakly Binding Form in the Dark. The previous section examined the optimal parameters for membranes containing photoactive carriers that are predominately in the strongly binding form in the dark. In this section, we explore the behavior of photofacilitated liquid membranes for which the carrier is predominantly in the weakly binding form in the dark. For this section, the definitions of the interconversion equilibria become

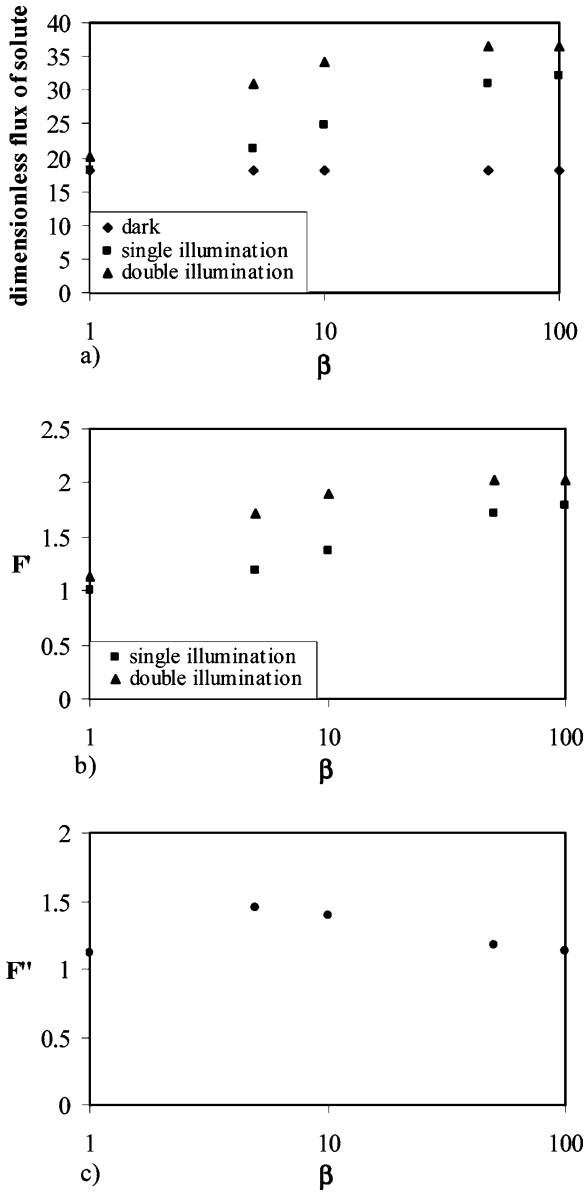

Figure 9. Plots of dimensionless flux of solute in the dark and under illumination, F' under double and single illumination, and F'' versus β for carriers that are predominantly in the strongly binding form in the dark. For all cases, $K_s^d = 10$, $K_w^d = 0.1$, $K_{caro} = 10$, $K_{como} = 1000$, $\alpha = 50$, $\epsilon_{caro} = \epsilon_{como} = 1.0$, and $\epsilon_s = \epsilon_w = 0.01$. Note that $\beta_{car,w} = \beta_{car,s} = \beta_{com,w} = \beta_{com,s}$ for all cases. (a) Plots of the dimensionless flux of solute versus β in the dark, under single illumination, and under double illumination. (b) Plots of the degree of photomodulation, F', versus β under single and double illumination. (c) Plot of the ratio of maximum solute flux under double illumination to the maximum solute flux under single illumination, F'', versus β.

$$B_s \underset{k_{-3}+k_{B_w}(I_w)}{\overset{k_3+k_{B_s}(I_s)}{\rightleftharpoons}} B_w$$

$$K_{car}(I) = \frac{k_3 + k_{B_s}(I_s)}{k_{-3} + k_{B_w}(I_w)} = K_{caro}\left(\frac{1 + \eta_{car,s}\bar{I}_s}{1 + \eta_{car,w}\bar{I}_w}\right) \quad (51)$$

where

$$K_{caro} = \frac{k_3}{k_{-3}} = \frac{[B_w]}{[B_s]}$$

$$\eta_{car_s} = \frac{\Phi_{B_s} E_{B_s} I_{o,s}}{k_3} \qquad (52)$$

$$\eta_{car_w} = \frac{\Phi_{B_w} E_{B_w} I_{o,w}}{k_{-3}}$$

and

$$AB_s \underset{k_{-4}+k_{AB_{ws}}(I_w)}{\overset{k_4+k_{AB_s}(I_s)}{\rightleftharpoons}} AB_w$$

$$K_{com}(I) = \frac{k_4 + k_{AB_s}(I_s)}{k_{-4} + k_{AB_w}(I_w)} = K_{como}\left(\frac{1 + \eta_{com,s}\bar{I}_s}{1 + \eta_{com,w}\bar{I}_w}\right) \qquad (53)$$

where

$$K_{como} = \frac{k_4}{k_{-4}} = \frac{[AB_w]}{[AB_s]}$$

$$\eta_{com_s} = \frac{\Phi_{AB_s} E_{AB_s} I_{o,s}}{k_4}$$

$$\eta_{car_w} = \frac{\Phi_{AB_w} E_{AB_w} I_{o,w}}{k_{-4}} \qquad (54)$$

The definitions of all other dimensionless parameters remain the same.

Effects of ϵ_{caro} and ϵ_{como}. For this section, ϵ_{caro} and ϵ_{como} are inversely related to the rate constants for the conversion of the weakly binding forms of the carrier and complex to the strongly binding forms in the dark, respectively. As in the previous section, increasing light intensity increases the rate at which the carriers convert between forms. Figure 10a shows that solute flux decreases under single illumination as ϵ_{caro} and ϵ_{como} increase (i.e., as the rate constants for carrier interconversion decrease), while the flux stays constant and high under double illumination. The values for F' stay fairly constant with increasing ϵ_{caro} and ϵ_{como} under single illumination, while increasing before leveling off under double illumination (Figure 10b). F'' also gradually increases then levels off with increasing ϵ_{caro} and ϵ_{como}, as shown in Figure 10c.

These trends are roughly similar to those seen for carriers that are predominantly in the strongly binding form in the dark (see Figure 2), and solute fluxes are about the same under double illumination whether the carrier is predominantly in the weakly or strongly binding form in the dark. However, there are some interesting differences. Carriers that are predominantly in the weakly binding form in the dark show higher fluxes with increasing ϵ_{caro} and ϵ_{como} under single illumination than do carriers that are predominantly in the strongly binding form in the dark. As ϵ_{caro} and ϵ_{como} increase, the carrier takes much longer to convert back to the form predominant in the dark and so tends to stay in the photoconverted form under single illumination. For carriers that are predominantly in the strongly binding form in the dark, the photoconverted form is the weakly binding form, so the membrane contains mostly poorly binding carrier under single illumination. As a result, solute fluxes are about the same as those in the dark (see Figure 2) which in turn produces low F' values. For carriers that are predominantly in the weakly binding form in the dark, photoconversion under single illumination results in the strongly binding form of the carrier, making a membrane with a fairly good carrier that can still maintain solute fluxes higher than those obtained in the dark. Under double illumination, light overcomes the slow carrier interconversion kinetics and membrane behavior is about the same regardless of what the carrier is like in the dark or the interconversion kinetics.

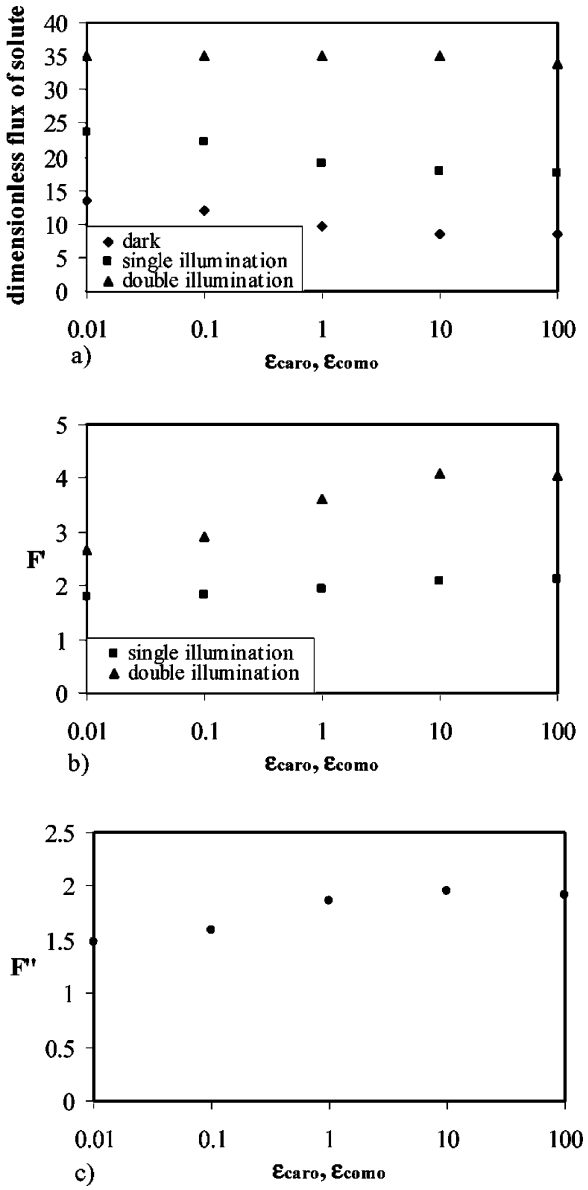

Figure 10. Plots of dimensionless flux of solute in the dark and under illumination, F' under double and single illumination, and F'' versus ϵ_{caro} and ϵ_{como} for carriers that are predominantly in the weakly binding form in the dark. For all cases, $K_s^d = 10$, $K_w^d = 0.1$, $K_{caro} = 10$, $K_{como} = 1000$, $\alpha = 50$, $\beta_{car,w} = \beta_{car,s} = \beta_{com,w} = \beta_{com,s} = 10$, and $\epsilon_s = \epsilon_w = 0.01$. (a) Plots of the dimensionless flux of solute versus ϵ_{caro} and ϵ_{como} in the dark, under single illumination, and under double illumination. (b) Plots of the degree of photomodulation, F', versus ϵ_{caro} and ϵ_{como} under single and double illumination. (c) Plot of the ratio of maximum solute flux under double illumination to the maximum solute flux under single illumination, F'', versus ϵ_{caro} and ϵ_{como}.

The beneficial effects of double illumination level off at ϵ_{caro} and ϵ_{como} values of 1.0 and higher, as shown by the values of F'' in Figure 10c. Consequently, we decided to run further simulations at ϵ_{car} and ϵ_{com} values of 1.0.

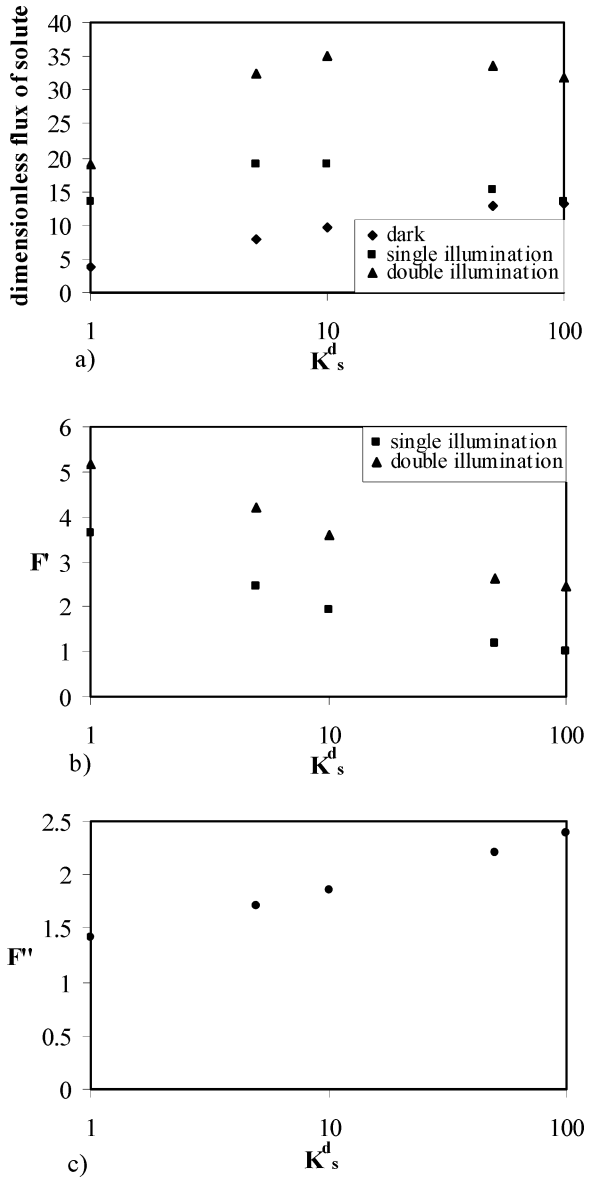

Figure 11. Plots of dimensionless flux of solute in the dark and under illumination, F' under double and single illumination, and F'' versus K_s^d for carriers that are predominantly in the weakly binding form in the dark. For all cases, $K_{caro} = 10$, $K_{como} = 1000$, $\alpha = 50$, $\beta_{car,w} = \beta_{car,s} = \beta_{com,w} = \beta_{com,s} = 10$, $\epsilon_{caro} = \epsilon_{como} = 1.0$, and $\epsilon_s = \epsilon_w = 0.01$. The ratio of K_s^d/K_w^d is held constant at 100. (a) Plots of the dimensionless flux of solute versus K_s^d in the dark, under single illumination, and under double illumination. (b) Plots of the degree of photomodulation, F', versus K_s^d under single and double illumination. (c) Plot of the ratio of maximum solute flux under double illumination to the maximum solute flux under single illumination, F'', versus K_s^d.

Effects of K_s^d and K_w^d. To explore the effects of binding equilibrium constants on transport behavior, K_s^d was varied between 100 and 1, while K_w^d was varied between 1 and 0.01. As in section 1, the ratio of K_s^d to K_w^d was kept constant at 100. Figure 11a shows that solute flux under both double and single illumination increases with increasing K_s^d and then begins to decrease at values of K_s^d greater than 10. Solute flux under double illumination is greater than that under single illumination such that F'' increases with increasing K_s^d as shown in Figure 11c. However, solute flux in the dark increases steadily with increasing K_s^d. Consequently, F' values under both double and single illumination decrease with increasing values of K_s^d, as shown in Figure 11b. We chose to conduct further simulations with a K_s^d value of 10, since that provides high solute flux under double illumination with reasonably high values of F' and F''.

The overall trends in the values of solute flux, F', and F'' with increasing value of K_w^d are very similar for carriers that are predominantly in the weakly binding form in the dark and for carriers that are predominantly in the strongly binding form in the dark, and Figure 5 applies qualitatively to both types of carrier.

For faster interconversion kinetics, the trends for the different types of carriers are quite different. As noted in section 1, many of the benefits of double illumination are lost for carriers with fast interconversion kinetics (ϵ_{caro} and ϵ_{como} values of 0.01 or less) when the carrier is predominantly in the strongly binding form in the dark. In contrast, for carriers that are predominantly in the weakly binding form in the dark, double illumination still provides significantly enhanced solute flux and F' values for carriers with fast interconversion kinetics, although the degree of enhancement decreases with increasing interconversion rate constants.

The improvement in performance under double illumination appears to level off for values of K_w^d less than 0.01. On the basis of these results, we chose to test other parameters keeping K_s^d at 10 and K_w^d at 0.01.

Effects of K_{caro} and K_{como}. As in the previous section, we only looked explicitly at the trends as a function of K_{caro} and defined K_{como} using eq 48. Figure 12a shows that solute flux remains fairly constant with increasing K_{caro} under double illumination but increases slightly under single illumination. Solute flux in the dark decreases steadily with increasing K_{caro}; consequently, as K_{caro} increases, F' increases under both double and single illumination, as shown in Figure 12b. The enhancement in solute transport under double illumination begins to level off at K_{caro} values of 10 and higher, while it continues to increase under single illumination. This results in a gradual decrease in values of F'' with increasing values of K_{caro} as shown in Figure 12c. As with trends in membrane performance with the value of K_w^d, trends in solute flux and F'' with K_{caro} follow similar patterns whether the carriers are predominantly in the strongly binding or weakly binding forms in the dark.

We chose to conduct further studies with a K_{caro} value of 10, since that value corresponds to high solute flux and fairly high values of F' and F''.

Effects of α. The trends in α for carriers that are predominantly in the weakly binding form in the dark are very similar to the trends seen for carriers that are predominantly in the strongly binding form in the dark, including a decline in F'' at faster interconversion kinetics than ϵ_{car} and ϵ_{com} values of 1.0. The trends depicted in Figure 7 and the discussion relating to Figure 7 apply qualitatively to both types of carrier. High values of α (10 or greater) are necessary for good membrane performance regardless of whether the carrier is predominantly in the strongly or weakly binding form in the dark.

Effects of β. As in section 1, we have chosen to set all values of β equal to each other to explore trends in membrane performance as a function of β. Figure 13a shows that solute flux increases steadily as β increases for both doubly and singly illuminated membranes while solute flux in the dark remains constant. This results in an increase in the photomodulation factor F' with increasing β under both single and double illumination (Figure 13b). F'' also increases as β increases from 1 to 10 and then levels off and even declines slightly at values of β greater than 10 (Figure 13c). Again, this behavior is almost the same for carriers that are predominantly in the strongly

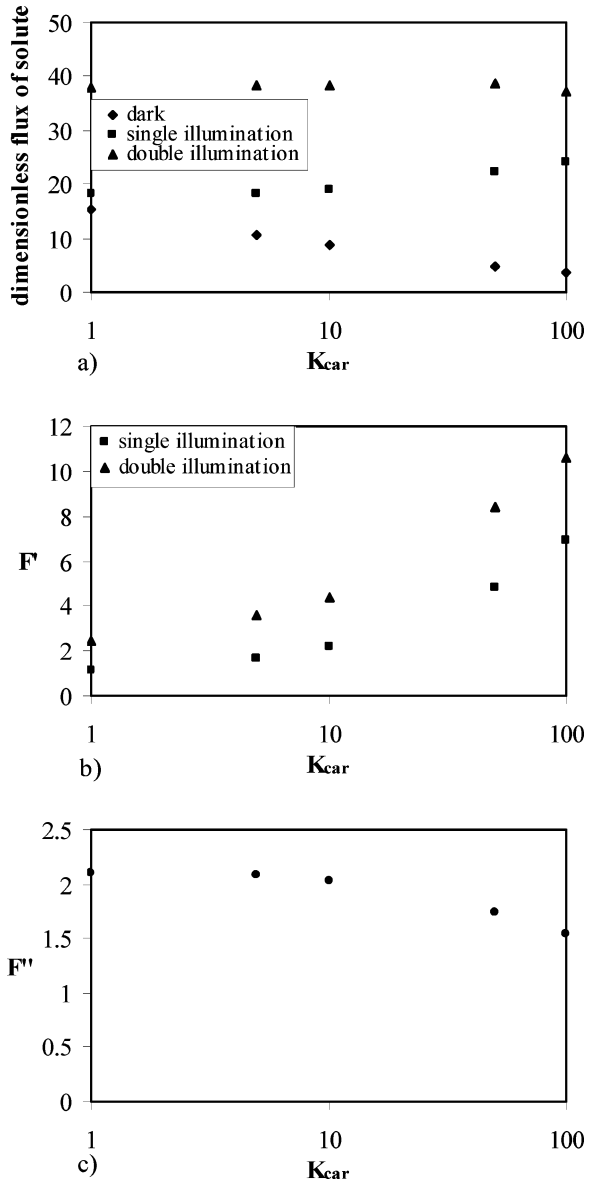

Figure 12. Plots of dimensionless flux of solute in the dark and under illumination, F' under double and single illumination, and F'' versus K_{caro} for carriers that are predominantly in the weakly binding form in the dark. For all cases, $K_s^d = 10$, $K_w^d = 0.01$, $\alpha = 50$, $\beta_{car,w} = \beta_{car,s} = \beta_{com,w} = \beta_{com,s} = 10$, $\epsilon_{caro} = \epsilon_{como} = 1.0$, and $\epsilon_s = \epsilon_w = 0.01$. (a) Plots of the dimensionless flux of solute versus K_{caro} in the dark, under single illumination, and under double illumination. (b) Plots of the degree of photomodulation, F', versus K_{caro} under single and double illumination. (c) Plot of the ratio of maximum solute flux under double illumination to the maximum solute flux under single illumination, F'', versus K_{caro}.

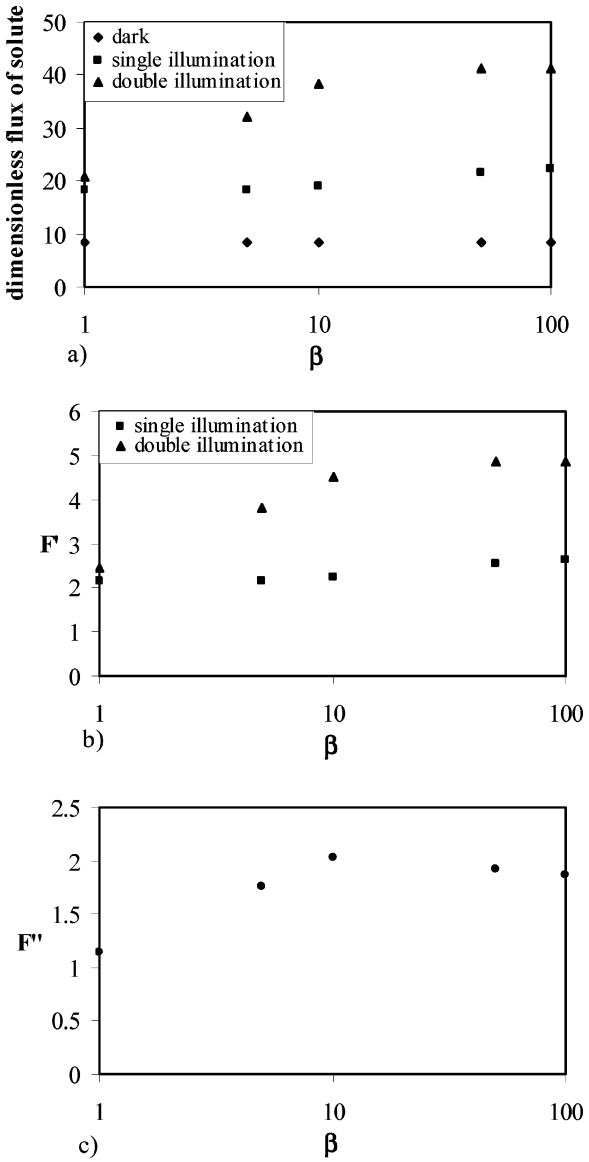

Figure 13. Plots of dimensionless flux of solute in the dark and under illumination, F' under double and single illumination, and F'' versus β for carriers that are predominantly in the weakly binding form in the dark. For all cases, $K_s^d = 10$, $K_w^d = 0.01$, $K_{caro} = 10$, $K_{como} = 10000$, $\alpha = 50$, $\epsilon_{caro} = \epsilon_{como} = 1.0$, and $\epsilon_s = \epsilon_w = 0.01$. Note that $\beta_{car,w} = \beta_{car,s} = \beta_{com,w} = \beta_{com,s}$ for all cases. (a) Plots of the dimensionless flux of solute versus β in the dark, under single illumination, and under double illumination. (b) Plots of the degree of photomodulation, F', versus β under single and double illumination. (c) Plot of the ratio of maximum solute flux under double illumination to the maximum solute flux under single illumination, F'', versus β.

binding form in the dark. On the basis of these results, a moderate β (between 10 and 100) is desirable.

Effects of ϵ_s and ϵ_w. As expected, increasing values of ϵ_s and ϵ_w (meaning decreasing values in the decomplexation rate constants) result in decreases in solute flux in the dark, under single illumination, and under double illumination. At high values of ϵ_s and ϵ_w (values greater than 1), solute fluxes under both double and single illumination are essentially the same as solute flux in the dark, meaning illumination does nothing to overcome slow decomplexation kinetics. This trend was also observed for carriers that are predominantly in the strongly binding form in the dark. As in section 1, values of ϵ_s and ϵ_w should be small (less than 1) for optimal membrane performance.

Section 3: Light Intensity. The role of light intensity in solute transport for doubly illuminated photofacilitated membranes has not yet been discussed. Under single illumination, for a given set of membrane and carrier properties, there is a well-defined light intensity that will produce maximum solute flux. Under double illumination, the light intensities needed for optimum solute flux are not so obvious. As described in the Simulation Methodology section, the light intensities on each side of the membrane are gradually increased until the increase in solute flux begins to level off, and the flux at that point is called the maximum flux. This is a somewhat arbitrary value, so the light intensities needed for maximum flux under double illumination are also somewhat arbitrary. However, some trends are clear.

Figure 14 shows an example of typical normalized light intensity profiles and normalized free solute concentration at maximum solute flux under double illumination. While these

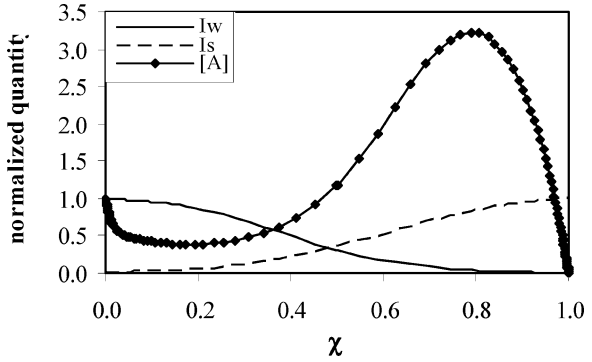

Figure 14. Normalized light intensity profiles for I_s (intensity of light at the wavelength that converts the strongly binding forms of the carrier and complex to the weakly binding forms), I_w (intensity of light at the wavelength that converts the weakly binding forms of the carrier and complex to the strongly binding forms), and normalized free solute concentration ([A]) as a function of normalized distance across the membrane. These profiles are for a carrier that is predominantly in the weakly binding form in the dark with the following properties: $K^d_s = 10$, $K^d_w = 0.01$, $K_{caro} = 10$, $K_{como} = 10000$, $\alpha = 50$, $\beta_{car,w} = \beta_{car,s} = \beta_{com,w} = \beta_{com,s} = 10$, $\epsilon_{caro} = \epsilon_{como} = 1.0$, $\epsilon_s = \epsilon_w = 0.01$.

profiles are for a membrane in which the carrier is predominantly in the weakly binding form in the dark, carriers that are predominantly in the strongly binding form in the dark produce very similar profiles at maximum solute flux. Indeed, normalized light intensity profiles at maximum solute flux look very similar regardless of carrier properties. In general, the normalized light intensity on each side remains high for a short distance into the membrane then falls off in an approximately exponential curve. Invariably, I_w falls to zero at the sweep interface and I_s falls to zero at the feed interface, while the light intensity profiles cross approximately halfway across the membrane. Normalized free solute concentration tends to reach a maximum two-thirds to three-quarters of the way across the membrane and can be much higher than the free solute concentration just inside the membrane at the feed interface. Note that these profiles are for normalized light intensities, where the actual light intensities have been normalized by the incident light intensities. Actual values of incident light intensities $I_{s,o}$ and $I_{w,o}$ will tend to be significantly different from each other as described below.

Significantly higher incident light intensities ($I_{s,o}$ and $I_{w,o}$) are needed to achieve maximum solute flux under double illumination than under single illumination. For carriers that are predominantly in the strongly binding form in the dark, the optimal incident light intensity needed to convert the strongly binding forms of the carrier and complex to the weakly binding forms at the sweep interface ($I_{s,o}$) is a factor of 5 to 10 times greater under double illumination than under single illumination. The optimal incident light intensity needed to convert the weakly binding forms of the carrier and complex to the strongly binding forms at the feed interface ($I_{w,o}$) is significantly lower than $I_{s,o}$. Since flux is only about a factor of 2 greater under double illumination than under single illumination while the light intensities needed to produce the optimal flux are much greater, double illumination is less photoefficient than single illumination.

Trends are slightly different for carriers that are predominantly in the weakly binding form in the dark. The optimal incident light intensity needed to convert the weakly binding forms of the carrier and complex to the strongly binding forms at the feed interface ($I_{w,o}$) under single illumination is generally an order of magnitude lower if the carrier is predominantly in the weakly binding form in the dark than if it is predominantly in the strongly binding form in the dark. This trend was observed

TABLE 1: Ranges of Parameter Values for Optimal Transport for Carriers Predominantly in the Strongly Binding Form in the Dark

	optimal flux and F' under illumination		
parameter	single	double	optimal F''
ϵ_{car}, ϵ_{com}	small (<1)	doesn't matter	large (≥1)
K_s^d	large (>10)	large (>10)	moderate (1−10)
K_w^d	small (<1)	small (<1)	small (<1)
K_{car}	large (>10)	doesn't matter	moderate (5−10)
α	large (>10)	large (>10)	large (>10)
β	large (≥10)	large (≥10)	moderate (5−10)
ϵ_s, ϵ_w	small (<1)	small (<1)	small (<1)

TABLE 2: Ranges of Parameter Values for Optimal Transport for Carriers Predominantly in the Weakly Binding Form in the Dark

	for optimal flux, F' under illumination		
parameter	single	double	optimal F''
ϵ_{car}, ϵ_{com}	small (<1)	doesn't matter	large (≥1)
K_s^d	moderate (5−10)	moderate (5−10)	large (≥10)
K_w^d	small (<0.1)	small (<0.1)	small (<0.1)
K_{car}	large (>10)	doesn't matter	moderate (5−10)
α	large (>10)	large (>10)	large (>10)
β	moderate to large (≥10)	moderate to large (≥10)	moderate to large (≥10)
ϵ_s, ϵ_w	small (<1)	small (<1)	small (<1)

in previous work exploring simulations of photofacilitated liquid membranes.[22,23] If the carrier is predominantly in the weakly binding form in the dark, the value of $I_{w,o}$ needed to obtain maximum solute flux under double illumination is generally at least 10 times greater than that needed under single illumination, and can be up to 100 times greater. The value of $I_{s,o}$ needed to obtain maximum solute flux under double illumination is usually of the same order of magnitude as the optimal value of $I_{w,o}$. However, in most cases, optimal incident light intensities are much lower when the carrier is predominantly in the weakly binding form in the dark than when it is in the strongly binding form in the dark. In general, solute flux is enhanced by about a factor of 2.5 or less when the carrier is predominantly in the weakly binding form in the dark, so again double illumination is a much less photoefficient process than single illumination.

Conclusions

The tables below summarize trends and general carrier characteristics for optimal membrane performance. Table 1 lists ranges of parameter values required to obtain optimal solute flux and photomodulation (F') under single and double illumination as well as ranges for which double illumination is significantly better than single illumination (F'') for carriers that are predominantly in the strongly binding form in the dark. Table 2 lists similar trends for carriers that are predominantly in the weakly binding form in the dark.

The primary advantage to using double illumination rather than single illumination occurs for carriers with slow interconversion kinetics between the strongly and weakly binding forms. For such carriers, single illumination produces only a moderate improvement in flux over transport in the dark, while double illumination produces a significant improvement.

Ranges of optimal values for the various parameters are similar whether the carrier is predominantly in the weakly or strongly binding form in the dark. In general, for carriers that are predominantly in the strongly binding form in the dark, double illumination will produce solute fluxes up to two times

greater than will single illumination. For carriers that are predominantly in the weakly binding form in the dark, double illumination can produce fluxes more than two times greater than can single illumination. Maximum flux values as a function of carrier properties under double illumination are similar regardless of whether the carrier is primarily in the strongly or weakly binding form in the dark.

There are advantages to using a carrier that is predominantly in the weakly binding form in the dark. Such carriers show higher values of F' under both double and single illumination. In addition, carriers that are primarily in the weakly binding form in the dark show enhanced transport at lower light intensities than do carriers that are predominantly in the strongly binding form in the dark and so are more photoefficient.

Experimental studies exploring doubly illuminated photofacilitated liquid membranes have recently appeared in the literature.[25] The investigators used a spirobenzopyran containing a crown ether to transport lithium ions. They reported a 50% enhancement in flux under double illumination versus illumination of the feed side of the membrane alone. Unfortunately, the experimental results are difficult to compare to the predictions of our model since several important conditions such as membrane thickness and interconversion rate constants were not reported. However, the experimental results do indicate that double illumination can provide a significant improvement in solute transport over single illumination.

An additional example of a carrier and membrane transport system that is likely to perform much better under double than under single illumination recently appeared in a study by Goyette et al.[17] In the experiment, the investigators developed a membrane transport cell specifically designed to test predictions of a model for transport in singly illuminated photofacilitated liquid membranes. They used a photoactive crown ether originally developed by Shinkai et al.[15] as the carrier to selectively transport NaTFMS over LiTFMS and control the flux with light. The single illumination model predicted that transport under single illumination should be about nine times greater than that obtained in the dark; the investigators observed enhanced transport values of 7.4 and 4.6. Using the double illumination model described in this paper, we believe the membrane transport system developed by Goyette et al. should result in an order of magnitude greater flux under double illumination than under single illumination. The carrier used in the study had relatively slow interconversion kinetics, and the carrier concentration in the membrane was several orders of magnitude greater than the solute concentration, resulting in a very large value of α. The combination of these factors should result in the large predicted enhancement in the rate of solute transport under double illumination versus single illumination.

We have demonstrated that double illumination of photofacilitated liquid membranes will result in enhanced transport over single illumination for a wide range of carrier properties. The degree of enhancement can be a factor of 2 or greater, depending on the characteristics of the carrier and membrane system. These results should help make is easier to select a carrier from the range of photoactive molecules available in the literature or to help design and synthesize a novel carrier.

Acknowledgment. This work was supported by a grant from the donors of the Petroleum Research Fund, administered by the American Chemical Society (#35478-GB7).

References and Notes

(1) Kemena, L. L.; Noble, R. D.; Kemp, N. J. *J. Membr. Sci.* **1983**, *15*, 259.
(2) Halwachs, W.; Schugerl, K. *Int. Chem. Eng.* **1980**, *20*, 519.
(3) Way, J. D.; Noble, R. D.; Flynn, T. M.; Sloan, E. D. *J. Membr. Sci.* **1982**, *12*, 239.
(4) Meldon, J. H.; Stroeve, P.; Gregoire, C. E. *Chem. Eng. Commun.* **1982**, *16*, 263.
(5) Noble, R. D.; Koval, C. A.; Pellegrino, J. J. *Chem. Eng. Prog.* **1989**, 58.
(6) Yang, X. J.; Fane, A. G.; Soldenhoff, K. *Ind. Eng. Chem. Res.* **2003**, *42*, 392.
(7) Schultz, J. S. *Science* **1977**, 197.
(8) Shinkai, S.; Nakaji, T.; Ogawa, T.; Shigematsu, K.; Manabe, O. *J. Am. Chem. Soc.* **1981**, *103*, 111.
(9) Shinkai, S.; Minami, T.; Kusano, Y.; Manabe, O. *J. Am. Chem. Soc.* **1982**, *104*, 1967.
(10) Shinkai, S.; Shigematsu, K.; Kusano, Y.; Manabe, O. *J. Chem. Soc., Perkin Trans. 1* **1981**, 3279.
(11) Shinkai, S.; Shigematsu, K.; Sato, M.; Manabe, O. *J. Chem. Soc., Perkin Trans. 1* **1982**, 2735.
(12) Shimidzu, T.; Yoshikawa, M. *J. Membr. Sci.* **1983**, *13*, 1.
(13) Irie, M.; Kato, M. *J. Am. Chem. Soc.* **1985**, *107*, 1024.
(14) Sasaki, H.; Ueno, A.; Osa, T. *Chem. Lett.* **1986**, 1785.
(15) Shinkai, S.; Miyazaki, K.; Manabe, O *J. Chem. Soc., Perkin Trans. 1* **1987**, 449.
(16) Haberfield, P. *J. Am. Chem. Soc.* **1987**, *109*, 6178.
(17) Goyette, M. L.; Longin, T. L.; Noble, R. D.; Koval, C. A. *J. Membr. Sci.* **2003**, *212*, 225.
(18) Jain, R.; Schultz, J. S. *J. Membr. Sci.* **1986**, *26*, 313.
(19) Sasaki, H.; Ueno, A.; Osa, T. *Bull. Chem. Soc. Jpn.* **1988**, *61*, 2321.
(20) Ino, M.; Otsuki, J.; Araki, K.; Seno, M. *J. Membr. Sci.* **1994**, *89*, 101.
(21) Jain, R.; Schultz, J. S. *J. Membr. Sci.* **1983**, *15*, 63.
(22) Longin, T. L.; Koval, C. A.; Noble, R. D. *J. Phys. Chem.* **1997**, *101*, 7172.
(23) Longin, T. L.; Koval, C. A.; Noble, R. D. *J. Phys. Chem.* **1998**, *102*, 1036.
(24) Longin, T. L.; Koval, C. A.; Noble, R. D. *J. Phys. Chem.* **1998**, *102*, 2064.
(25) Sakamoto, H.; Takagaki, H.; Nakamura, M.; Kimura, K. *Anal. Chem.* **2005**, *77*, 1999.
(26) Alfimov, M. V.; Fedorov, Y. V.; Fedorova, O. A.; Gromov, S. S.; Hester, R. E.; Lednev, I. K.; Moore, J. N.; Oleshko, V. P.; Vedernikov, A. I. *J. Chem. Soc., Perkin Trans. 2* **1996**, 1441.
(27) Fedorova, O. A.; Gromov, S. P.; Alfimov, M. V. *Dokl. Akad. Nauk* **1995**, *341*, 219.
(28) Feofanov, A. V.; Ianoul, A. I.; Oleinikov, V. A.; Naviev, I. R.; Gromov, S. P.; Fedorova, O. A.; Alfimov, M. V. *Russ. Chem. Bull.* **1995**, *44*, 2323.
(29) Gromov, S. P.; Golosov, A. A.; Fedorova, O. A.; Levin, D. E.; Alfimov, M. V. *Russ. Chem. Bull.* **1995**, *44*, 124.
(30) Alfimov, M. V.; Gromov, S. P.; Nazarov, V. B.; Pilyugina, O. M.; Fomina, M. V. *Dokl. Akad. Nauk* **1993**, *330*, 453.
(31) Alfimov, M. V.; Kamalov, V. F.; Struganova, I. A.; Yoshihara, K. *Chem. Phys. Lett.* **1992**, *195*, 262.
(32) Alfimov, M. V.; Gromov, S. P.; Lednev, I. K. *Chem. Phys. Lett.* **1991**, *185*, 455.
(33) Shinkai, S.; Ogawa, T.; Kusano, Y.; Manabe, O. *Chem. Lett.* **1980**, 283.
(34) Yamashita, I.; Fujii, M.; Kaneda, T.; Misumi, S. *Tetrahedron Lett.* **1980**, *21*, 541.
(35) Smith, K. A.; Meldon, J. H.; Colton, C. K. *AIChE J.* **1973**, *19*, 102.